

New BER Expression of Hierarchical M-ary Phase Shift Keying

Jaeyoon Lee, Kyongkuk Cho, and Dongweon Yoon

In-phase/quadrature (I/Q) imbalances, which are generated by non-ideal transceiver components, are inevitable physical phenomena that cause the performance of practical communication systems to be degraded. In this paper, we provide a new closed-form expression for the bit error rate of hierarchical M-ary phase shift keying with I/Q phase and amplitude imbalances and analyze the effect of I/Q imbalances on BER performance over an additive white Gaussian noise channel.

Keywords: Hierarchical modulation, digital communication, BER.

I. Introduction

Hierarchical modulation divides transmitted messages into two or more classes and assigns each class a degree of reliability according to its importance [1]. The process exists to ensure that all receivers receive the most important information, and that only receivers with better reception conditions receive more inconsequential information [2]. In accordance with the increasing interest in digital video broadcasting (DVB) systems and wireless multimedia services, hierarchical modulation has recently been accepted as standard for DVB-T and DVB-S systems by ETSI [3]-[6].

There have been various studies of bit error rate (BER) expressions of hierarchical modulation schemes, such as hierarchical M-ary phase shift keying (H-MPSK) and hierarchical M-ary quadrature amplitude modulation (H-MQAM) [2], [7]-[10]. Specifically for H-MPSK, Alouini [2] derived the exact recursive BER expression with in-phase/quadrature (I/Q) balance using the Pawula function from [11]. In practical communication systems, BER performance is affected by imbalances in I/Q phase and amplitude, which are attributed to an imperfect 90-degree phase shifter and unequal filter gains, respectively [12]. Previous works have focused primarily on I/Q balance. However, a method was recently developed to obtain the error probabilities for an arbitrary two-dimensional (2-D) signal constellation with I/Q imbalances using the 2-D Gaussian Q-function [13]. Although the method provided in [13] is exact and general, its extension to the acquisition of a closed-form expression for average BER is more complex and time consuming.

The purpose of this paper is twofold. We first provide a new closed-form expression involving the 2-D Gaussian Q-function for the BER of H-MPSK. Then, we investigate the effect of I/Q

Manuscript received Jan. 05. 2007; revised Aug. 01. 2007.

Jaeyoon Lee (phone: +82 2 2220 0711, email: jylee1988@gmail.com), Kyongkuk Cho (email: kyongkuk@gmail.com), and Dongweon Yoon (phone: + 82 2 2220 0362, email: dwyoon@hanyang.ac.kr) are with the Department of Electronics and Computer Engineering, Hanyang University, Seoul, Rep. of Korea.

phase and amplitude imbalances on BER performance over an additive white Gaussian noise (AWGN) channel. First, we derive and analyze the BER expressions for the k -th bit of H-4/8/16PSK signal constellations when Gray code bit mapping is employed. Regular patterns of significant parameters in the k -th bit error probability are observed while the BER expression is developed. We then determine a function to simply generate a regular pattern, which is used to present a new average BER expression for H-MPSK with I/Q phase and amplitude imbalances. Finally, we analyze the effect of I/Q imbalances on BER performance.

II. System Model

In H-MPSK with $\Theta_M = [\theta_1 \theta_2 \dots \theta_{N-1}]$, $N = \log_2 M$, the highest priority bit is assigned to the most significant bit (MSB) position, and the lowest priority bit is located in the least significant bit (LSB) position. The highest priority bit yields the binary PSK constellation and the next priority bits yield the quadrature PSK (QPSK) constellation. The H-MPSK constellation is generated with increases in the number of signal points. As an example, Fig. 1 shows the H-8PSK signal constellation [2]. The symbols “ \times ” and “+” denote fictitious symbols, while “ \circ ” represents actual transmitted symbols; $2\theta_1$ represents the angle between the “+” symbols, which include the first and second priority bits that are centered around the fictitious “ \times ” symbols; and $2\theta_2$ represents the angle between the symbols in the H-8PSK constellation that are centered around the fictitious “+” symbols [2]. Additional angles, including θ_3 and θ_4 , will be introduced as the number of signal points is increased.

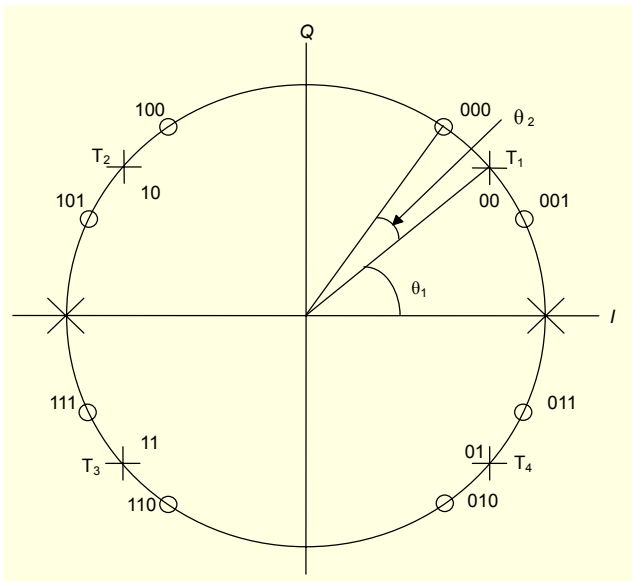


Fig. 1. H-8PSK signal constellation.

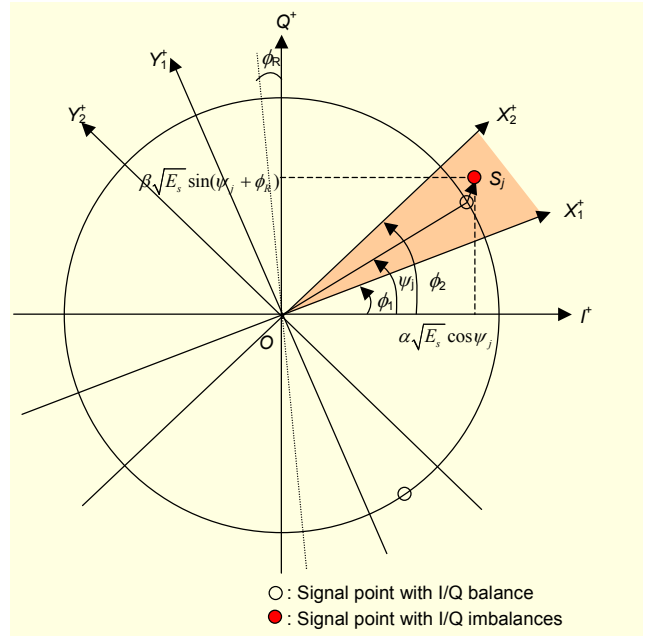


Fig. 2. Correct region for a signal point of H-MPSK with I/Q imbalances.

The transmitted signals are assumed to be Gray-encoded.

Figure 2 shows a signal point of H-MPSK with I/Q imbalances. To find an exact and general BER expression for the H-MPSK signal with I/Q imbalances, we use the two dimensional joint Gaussian Q-function [14]. The probability $P_{r-j} \{ \phi_1 \leq \Omega \leq \phi_2 \}$ that a signal point S_j falls into the shaded region in Fig. 2 can be obtained, as given in [15], as

$$P_{r-j} \{ \phi_1 \leq \Omega \leq \phi_2 \} = P_{r-j} \{ \angle X_1^+ O X_2^+ \} = P_{r-j} \{ Y_1 \geq 0, Y_2 \leq 0 \} \\ = Q \left(-\frac{E[Y_1]}{\sqrt{\text{Var}[Y_1]}}, \frac{E[Y_2]}{\sqrt{\text{Var}[Y_2]}}; -\rho_{Y_1 Y_2} \right), \quad (1)$$

where ϕ_1 and ϕ_2 are the angles between I' and X_i' ($i=1, 2$). In Fig. 2, Y_1 and Y_2 have joint Gaussian distribution, as given in [13], with

$$E[Y_i] = \sqrt{E_s} \left(\beta \cos \phi_i \sin(\psi_j + \phi_R) - \alpha \sin \phi_i \cos \psi_j \right), \quad i=1, 2, \\ \text{VAR}[Y_i] = \sigma^2 \left(\alpha^2 \sin^2(\phi_i) + \beta^2 \cos^2(\phi_i) - \alpha\beta \sin \phi_R \sin(2\phi_i) \right), \quad i=1, 2, \\ \rho_{Y_1 Y_2} = \frac{\text{COV}[Y_1 Y_2]}{\sqrt{\text{VAR}[Y_1]} \sqrt{\text{VAR}[Y_2]}} \\ = \frac{\sigma^2 \left(\alpha^2 \sin \phi_1 \sin \phi_2 + \beta^2 \cos \phi_1 \cos \phi_2 - \alpha\beta \sin \phi_R \sin(\phi_1 + \phi_2) \right)}{\sqrt{\text{VAR}[Y_1]} \sqrt{\text{VAR}[Y_2]}}, \quad (2)$$

where Y_i ($i=1, 2$) is perpendicular to the decision boundary X_i ($i=1, 2$); E_s is the symbol energy; ψ_j ($j=0, 1, 2, \dots, M-1$) is

the phase of the transmitted signal point; α and β are the I- and Q-channel filter gains, respectively [13]; ϕ_R represents the degree of I/Q phase imbalance; and $\rho_{IQ} = \sin \phi_R$ is the correlation coefficient of the I- and Q-channels [16].

In (2), the phase (ψ_j) and angle pair (ϕ_1, ϕ_2) vary with the position of the signal points. Therefore, we first obtain the phase (ψ_j) and angle pair (ϕ_1, ϕ_2) for the k -th bit of every transmitted signal point in H-4/8/16PSK. Then we observe the regular patterns resultant from phase and angle values being varied. From the patterns, we finally provide the exact and general BER expression of H-MPSK. We used a similar method to obtain the closed-form expression for the BER of uniform rectangular QAM [17].

III. Generalized BER Expression of H-MPSK

In this section, we first consider the signal constellations of H-4/8/16PSK with I/Q imbalances to determine the decision boundaries for the transmitted symbols and obtain the closed-form expressions for the BERs of H-4/8/16PSK with I/Q imbalances. Then, we generalize a new BER expression of H-MPSK with I/Q imbalances by analyzing the BER expressions of the k -th bit of H-4/8/16PSK.

1. H-4PSK

Figure 3 depicts the signal constellation of H-4PSK with I/Q phase and amplitude imbalances. As shown in the figure, in which s_j ($j=0, 1, 2, 3$) represent signal points, I/Q imbalances cause shifts in the signal points, alterations in the Euclidean-distance between points, and finally, degradations in the BER performance.

As stated previously, BER computation is contingent upon the identification of the phase (ψ_j) and angle pair (ϕ_1, ϕ_2) of each signal point. We define the phase vector as $\Psi_{H-MPSK} = [\psi_0 \ \psi_1 \ \dots \ \psi_{M-1}]$, which contains the phases of each signal point. The phase vector for H-4PSK is given as

$$\Psi_{H-4PSK} = [\theta_1 \ \pi - \theta_1 \ \pi + \theta_1 \ 2\pi - \theta_1]. \quad (4)$$

In this paper, we assume that the MSB is the first bit ($b_k, k=1$). Since the decision boundary varies with the k -th bit (b_k) in a symbol, the angle pairs (ϕ_1, ϕ_2) can be obtained as follows.

For the first bit (b_1), the decision boundary is simply the Q^+ axis. For instance, the error regions for the first bit of a signal point s_0 are 2- and 3- quadrants as shown in Fig. 3; therefore, the angle pair (ϕ_1, ϕ_2) for the first bit of s_0 is $(\pi/2, 3\pi/2)$. Consequently, when $k=1$, the angle pairs (ϕ_1, ϕ_2) for every signal point can be obtained as

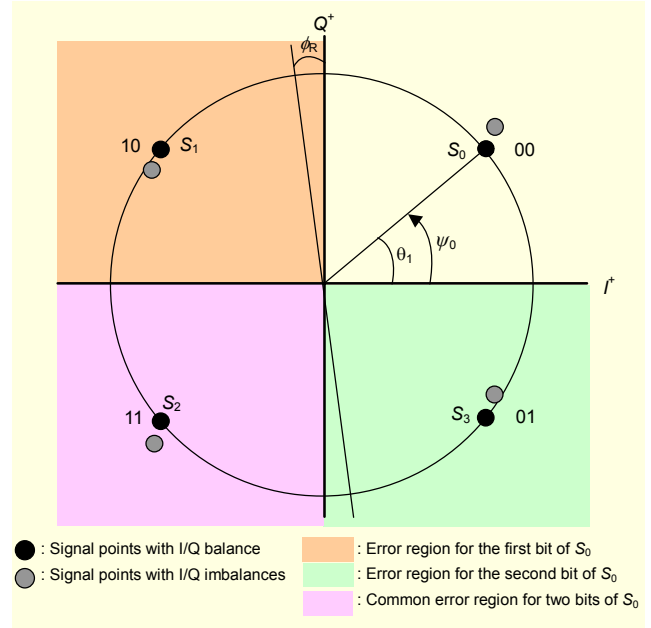


Fig. 3. H-4PSK signal constellation.

$$(\phi_1, \phi_2) = \begin{cases} \left(\frac{\pi}{2}, 3\pi/2 \right), & \text{when } b_1 = 0, \\ \left(3\pi/2, 5\pi/2 \right), & \text{when } b_1 = 1. \end{cases} \quad (5)$$

For the second bit ($b_k, k=2$), the decision boundary is the I^+ axis. The error regions for the second bit of signal point s_0 are 3- and 4-quadrants as shown in Fig. 3. Thus, when $k=2$, the angle pairs (ϕ_1, ϕ_2) for every signal point can be obtained as

$$(\phi_1, \phi_2) = \begin{cases} \left(\frac{\pi}{2}, 2\pi \right), & \text{when } b_2 = 0, \\ \left(0, \pi \right), & \text{when } b_2 = 1. \end{cases} \quad (6)$$

The BER of H-4PSK can simply be computed using (1) and (2) with the angles determined in (5) and (6).

2. H-8PSK

The results from the case of H-4PSK can be extended to H-8PSK. In the case of H-8PSK, we have 3 bits per symbol. Figure 4 shows the signal constellation of H-8PSK with $\Theta_8 = [\theta_1 \ \theta_2]$ in the presence of I/Q phase and amplitude imbalances. The phase vector for H-8PSK is given as

$$\begin{aligned} \Psi_{H-8PSK} &= [\psi_0 \ \psi_1 \ \dots \ \psi_7] \\ &= [\theta_1 - \theta_2 \quad \theta_1 + \theta_2 \quad \pi - \theta_1 - \theta_2 \quad \pi - \theta_1 + \theta_2 \\ &\quad \pi + \theta_1 - \theta_2 \quad \pi + \theta_1 + \theta_2 \quad 2\pi - \theta_1 - \theta_2 \quad 2\pi - \theta_1 + \theta_2]. \end{aligned} \quad (7)$$

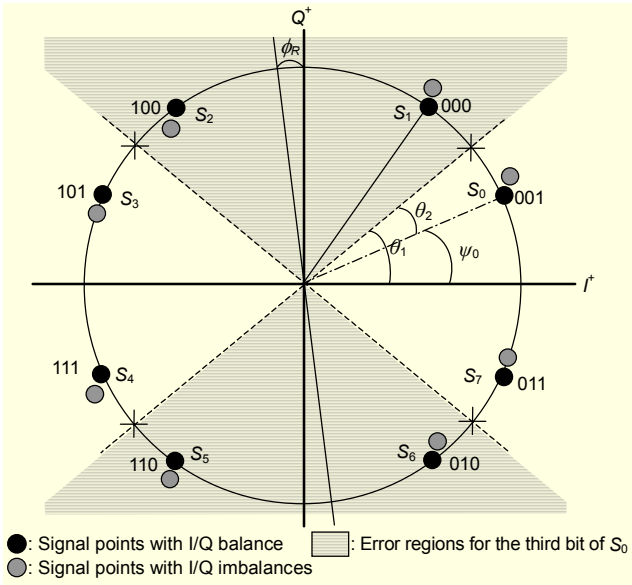


Fig. 4. H-8PSK signal constellation.

The angle pairs (ϕ_1, ϕ_2) for the decision boundaries corresponding to each bit can be obtained as follows.

For the first bit (b_1) and the second bit (b_2), the decision boundaries are identical to those of H-4PSK. Therefore, the angle pairs (ϕ_1, ϕ_2) of both bits for every signal point are as given in (5) and (6).

For H-8PSK, there are two separate regions of the third bit ($b_k, k=3$), which together result in its incorrect detection. For example, as shown in Fig. 4, two error regions exist for the third bit of s_0 . Let l be the number of separate regions. The error probability that a received signal falls into one of the separate regions can be obtained using a 2-D Gaussian Q-function. Another 2-D Gaussian Q-function can be used to obtain the error probability of other regions. Accordingly, l implies the number of 2-D Gaussian Q-functions required to determine the error probability of a signal. In H-8PSK, $l=2$. Therefore, unlike the first and second bits, two angle pairs (ϕ_1, ϕ_2) determine the decision regions of the third bit, which are given as

$$\begin{pmatrix} \phi_1 \\ \phi_2 \end{pmatrix} = \begin{cases} \begin{pmatrix} \theta_1 \\ \pi - \theta_1 \end{pmatrix} \text{ or } \begin{pmatrix} \pi + \theta_1 \\ 2\pi - \theta_1 \end{pmatrix}, & \text{when } b_3 = 1, \\ \begin{pmatrix} \pi - \theta_1 \\ \pi + \theta_1 \end{pmatrix} \text{ or } \begin{pmatrix} 2\pi - \theta_1 \\ 2\pi + \theta_1 \end{pmatrix}, & \text{when } b_3 = 0. \end{cases} \quad (8)$$

The BER for H-8PSK can be expressed in terms of two 2-D Gaussian Q-functions by using (1) and (2) with the angles determined by (5), (6), and (8).

3. H-16PSK

For H-16PSK, we have 4 bits per symbol. Figure 5 shows

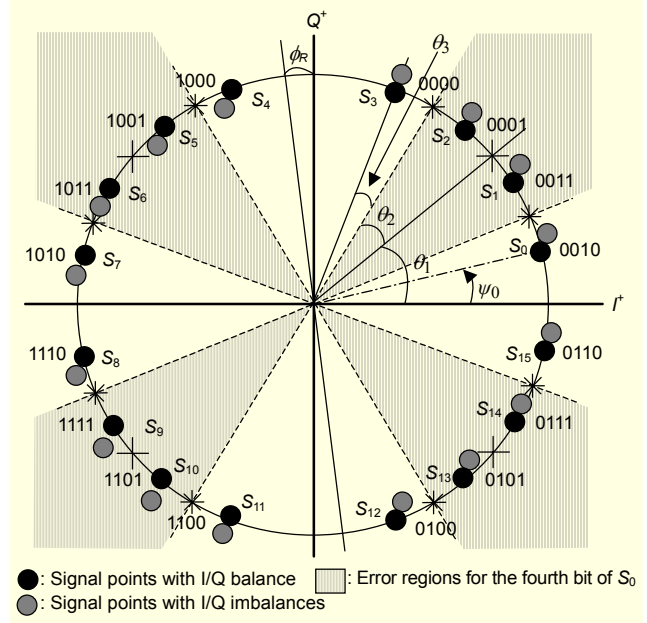


Fig. 5. H-16PSK signal constellation.

the signal constellation of H-16PSK with $\Theta_{16} = [\theta_1 \ \theta_2 \ \theta_3]$ in the presence of I/Q imbalances. The phase vector of the signal points of H-16PSK is

$$\begin{aligned} \Psi_{H-16PSK} &= [\psi_0 \ \psi_1 \ \dots \ \psi_{15}] \\ &= [\theta_1 - \theta_2 - \theta_3 \quad \theta_1 - \theta_2 + \theta_3 \quad \theta_1 + \theta_2 - \theta_3 \quad \theta_1 + \theta_2 + \theta_3 \\ &\quad \pi - \theta_1 - \theta_2 - \theta_3 \quad \pi - \theta_1 - \theta_2 + \theta_3 \quad \pi - \theta_1 + \theta_2 - \theta_3 \quad \pi - \theta_1 + \theta_2 + \theta_3 \\ &\quad \pi + \theta_1 - \theta_2 - \theta_3 \quad \pi + \theta_1 - \theta_2 + \theta_3 \quad \pi + \theta_1 + \theta_2 - \theta_3 \quad \pi + \theta_1 + \theta_2 + \theta_3 \\ &\quad 2\pi - \theta_1 - \theta_2 - \theta_3 \quad 2\pi - \theta_1 - \theta_2 + \theta_3 \quad 2\pi - \theta_1 + \theta_2 - \theta_3 \quad 2\pi - \theta_1 + \theta_2 + \theta_3]. \end{aligned} \quad (9)$$

The angle pairs (ϕ_1, ϕ_2) for the BER computation of the first three bits ($b_k, k=1, 2, 3$) are identical to the angles found in H-8PSK, and they are shown in (5), (6), and (8), respectively.

For the fourth bit ($b_k, k=4$), as shown in Fig. 5, there are four separate regions ($l=4$) resulting in incorrect detection of the fourth bit in H-16PSK. Thus, the four angle pairs corresponding to the four regions are given as

$$\begin{pmatrix} \phi_1 \\ \phi_2 \end{pmatrix} = \begin{cases} \begin{pmatrix} \theta_1 - \theta_2 \\ \theta_1 + \theta_2 \end{pmatrix}, \begin{pmatrix} \pi - \theta_1 - \theta_2 \\ \pi - \theta_1 + \theta_2 \end{pmatrix}, \begin{pmatrix} \pi + \theta_1 - \theta_2 \\ \pi + \theta_1 + \theta_2 \end{pmatrix}, \text{ or } \begin{pmatrix} 2\pi - \theta_1 - \theta_2 \\ 2\pi - \theta_1 + \theta_2 \end{pmatrix}, & \text{when } b_4 = 0 \\ \begin{pmatrix} \theta_1 + \theta_2 \\ \pi - \theta_1 - \theta_2 \end{pmatrix}, \begin{pmatrix} \pi - \theta_1 + \theta_2 \\ \pi + \theta_1 - \theta_2 \end{pmatrix}, \begin{pmatrix} \pi + \theta_1 + \theta_2 \\ 2\pi - \theta_1 - \theta_2 \end{pmatrix}, \text{ or } \begin{pmatrix} 2\pi - \theta_1 + \theta_2 \\ 2\pi + \theta_1 - \theta_2 \end{pmatrix}, & \text{when } b_4 = 1. \end{cases} \quad (10)$$

The BER of the fourth bit (b_4) can be computed with four 2-D Gaussian Q functions and the overall BER of H-16PSK

can be obtained using (1) and (2) with the angles determined in (5), (6), (8), and (10).

4. Regular Patterns in Developing BER Expression

As mentioned at the end of section II, the development of a generalized BER expression is contingent upon two parameters, namely, the phase (ψ_j) and angle pairs (ϕ_1, ϕ_2). These parameters vary with the transmitted signal points. From (4), (7), and (9), we set the generalized form for the elements of the phase vector $\Psi_{H-MPSK} = [\psi_0 \ \psi_1 \ \dots \ \psi_{M-1}]$ as

$$\psi_j = A_j \cdot \pi + \sum_{i=1}^{\log_2 M - 1} (-1)^{B_{i,j}} \cdot \theta_i, \quad j = 0, 1, 2, \dots, M-1, \quad (11)$$

where A_j and $B_{i,j}$ can be found by analyzing their regular patterns.

A. Regular Pattern of A_j

The regular pattern of A_j can be observed. As shown in Table 1, A_j terms have the values of 0, 1, and 2, which are repeated $2^{\log_2 M - 2}$, $2^{\log_2 M - 1}$, and $2^{\log_2 M - 2}$ times, respectively. The total number of A_j terms is equal to M , and as M doubles, the run-length of each term doubles where $*, *, \dots, *$ denotes the run. Finally, from these results, the function to generate the coefficient A_j for any M and j can be found by

$$A_j = \left\lfloor \frac{4j}{M} \right\rfloor - \left\lfloor \frac{2j}{M} \right\rfloor, \quad j = 0, 1, \dots, M-1, \quad (12)$$

where $\lfloor x \rfloor$ denotes the largest integer less than or equal to x .

Table 1. Regular pattern of the coefficient A_j .

M	$A_j, j = 0, 1, 2, \dots, M-1$
4	0 1 1 2
8	0 0 1 1 1 1 2 2
16	0 0 0 0 1 1 1 1 1 1 1 1 2 2 2 2
⋮	⋮

Table 2. Sign variations of θ_i .

M	$\theta_i, i = 1, 2, \dots, \log_2 M - 1$	$j = 0 \ 1 \ 2 \ 3 \ 4 \ 5 \ 6 \ 7 \ 8 \ 9 \ 10 \ 11 \ 12 \ 13 \ 14 \ 15 \ \dots \ M-1$
4	θ_1	$\pm \mp \pm \mp$
8	θ_1	$++ \text{---} ++ \text{---}$
	θ_2	$\text{---} + \text{---} + \text{---} + \text{---}$
16	θ_1	$++++ \text{---} \text{---} ++ \text{---} + \text{---} \text{---}$
	θ_2	$\text{---} + \text{---} \text{---} + \text{---} \text{---} + \text{---} \text{---} + \text{---}$
	θ_3	$\text{---} + \text{---} + \text{---} + \text{---} + \text{---} + \text{---} + \text{---} + \text{---}$
⋮	⋮	⋮

B. Regular Pattern of $B_{i,j}$

Table 2 shows the sign variations of θ_i . When $i=1$, the sign of θ_i begins with “+”. For other values of i , the signs of the first terms of θ_i starts with “-”. When $i=\log_2 M - 1$, the pattern of “- +” is repeated $M/2$ times. The run-length of the signs for the same value of i doubles as M increases twofold.

Table 3 shows the regular patterns of exponent $B_{i,j}$ required to determine the sign of θ_i . The first term of $B_{i,j}$ for i is

$$B_{i,j} = \begin{cases} 0, & i = 1, \\ 1, & i \neq 1, \end{cases} \quad (13)$$

and when $i=\log_2 M - 1$, the terms increase by 1 with j . The total number of terms is equal to M , and for the same value of i , the run-length of each term with exponent $B_{i,j}$ doubles as M increases twofold. Thus, from these properties, we can find a general expression for exponent $B_{i,j}$ for any M, i , and j :

$$B_{i,j} = \left\lfloor \frac{4j}{2^{\log_2 M + 1 - i}} \right\rfloor + 1 - \left\lfloor \frac{1}{i} \right\rfloor, \quad (14)$$

where $i = 1, 2, \dots, \log_2 M - 1$, and $j = 0, 1, \dots, M - 1$.

Consequently, the generalized form for the elements of the phase vector can be expressed as

$$\begin{aligned} \psi_j &= \pi \left(\left\lfloor \frac{4j}{M} \right\rfloor - \left\lfloor \frac{2j}{M} \right\rfloor \right) + \sum_{i=1}^{\log_2 M - 1} \theta_i \cdot (-1)^{\left\lfloor \frac{4j}{2^{\log_2 M + 1 - i}} \right\rfloor + 1 - \left\lfloor \frac{1}{i} \right\rfloor} \\ &= \Omega(M, j, \Theta), \end{aligned} \quad (15)$$

where $\Theta_M = (\theta_1, \theta_2, \dots, \theta_{\log_2 M - 1})$.

The angle pair for each bit of H-MPSK can be generalized by (15). For the first and second bits, the angle pairs corresponding to the j -th signal points (s_j) of H-MPSK can be rephrased as follows:

for b_1 ,

$$(\phi_1, \phi_2) = \begin{cases} \left(\begin{matrix} \pi/2 \\ 3\pi/2 \end{matrix} \right), & \text{when } b_1 = 0, \\ \left(\begin{matrix} 3\pi/2 \\ 5\pi/2 \end{matrix} \right), & \text{when } b_1 = 1, \end{cases} \quad (16)$$

for b_2 ,

$$(\phi_1, \phi_2) = \begin{cases} \left(\begin{matrix} \pi \\ 2\pi \end{matrix} \right), & \text{when } b_2 = 0, \\ \left(\begin{matrix} 0 \\ \pi \end{matrix} \right), & \text{when } b_2 = 1. \end{cases} \quad (17)$$

For other bits ($b_k, k \geq 3$), the angle pairs corresponding to the j -th signal points (s_j) can be expressed with the phase vector of H- 2^{k-1} PSK. Thus, according to bit values (0 or 1), the angle

Table 3. Regular pattern of B_{ij} .

M	$B_{ij}, i=1, 2, \dots, \log_2 M-1$	$B_{ij}, j=0, 1, 2; \dots, M-1$
4	B_{1j}	<u>0 1 2 3</u>
8	B_{1j}	<u>0 0 1 1 2 2 3 3</u>
	B_{2j}	<u>1 2 3 4 5 6 7 8</u>
16	B_{1j}	<u>0 0 0 0 1 1 1 1 2 2 2 2 3 3 3 3</u>
	B_{2j}	<u>1 1 2 2 3 3 4 4 5 5 6 6 7 7 8 8</u>
	B_{3j}	<u>1 2 3 4 5 6 7 8 9 10 11 12 13 14 15 16</u>
⋮	⋮	⋮
M	B_{1j}	<u>0 0 ⋯ 0 0 1 1 ⋯ 1 1 2 2 ⋯ 2 2 3 3 ⋯ 3 3</u>
	B_{2j}	<u>1 ⋯ 1 2 ⋯ 2 3 ⋯ 3 4 ⋯ 4 5 ⋯ 5 6 ⋯ 6 7 ⋯ 7 8 ⋯ 8</u>
	⋮	⋮
	$B_{\log_2 M-1 j}$	<u>1 2 3 4 5 6 7 8 9 10 11 ⋯</u> $\left\lfloor \frac{4j}{2^{\log_2 M-1-\log_2 M+1}} \right\rfloor + 1 - \left\lfloor \frac{1}{\log_2 M-1} \right\rfloor$

pairs can be obtained as follows:

for b_3 , and $n = 0, 1, \dots, l-1$,

$$\begin{pmatrix} \phi_1 \\ \phi_2 \end{pmatrix} = \begin{cases} \begin{pmatrix} \Psi_{2n|_{H-2^{k-1}PSK}} \\ \Psi_{2n+1|_{H-2^{k-1}PSK}} \end{pmatrix} = \begin{pmatrix} \Omega(2^{k-1}, 2n, \Theta_{2^{k-1}}) \\ \Omega(2^{k-1}, 2n+1, \Theta_{2^{k-1}}) \end{pmatrix}, & \text{when } b_3=1, \\ \begin{pmatrix} \Psi_{2n+1|_{H-2^{k-1}PSK}} \\ \Psi_{2n+2|_{H-2^{k-1}PSK}} \end{pmatrix} = \begin{pmatrix} \Omega(2^{k-1}, 2n+1, \Theta_{2^{k-1}}) \\ \Omega(2^{k-1}, 2n+2, \Theta_{2^{k-1}}) \end{pmatrix}, & \text{when } b_3=0; \end{cases} \quad (18)$$

for b_k ($k > 3$) and $n = 0, 1, \dots, l-1$,

$$\begin{pmatrix} \phi_1 \\ \phi_2 \end{pmatrix} = \begin{cases} \begin{pmatrix} \Psi_{2n|_{H-2^{k-1}PSK}} \\ \Psi_{2n+1|_{H-2^{k-1}PSK}} \end{pmatrix} = \begin{pmatrix} \Omega(2^{k-1}, 2n, \Theta_{2^{k-1}}) \\ \Omega(2^{k-1}, 2n+1, \Theta_{2^{k-1}}) \end{pmatrix}, & \text{when } b_k(k > 3)=0, \\ \begin{pmatrix} \Psi_{2n+1|_{H-2^{k-1}PSK}} \\ \Psi_{2n+2|_{H-2^{k-1}PSK}} \end{pmatrix} = \begin{pmatrix} \Omega(2^{k-1}, 2n+1, \Theta_{2^{k-1}}) \\ \Omega(2^{k-1}, 2n+2, \Theta_{2^{k-1}}) \end{pmatrix}, & \text{when } b_k(k > 3)=1, \end{cases} \quad (19)$$

where $\Omega(2^{k-1}, j, \Theta_{2^{k-1}})$ can be obtained from (15), and l denotes the number of 2-D Gaussian Q-functions determinable by

$$l = 2^{\lfloor \frac{k-2}{k} \rfloor}. \quad (20)$$

The above results for the angle pairs are based on the consistency of the bit format for a Gray-coded signal constellation.

5. Another Expression of Regular Patterns Using a Recursive Algorithm

In this subsection, we present another expression of regular patterns using a recursive algorithm. Consider the phase vector $\Psi_{H-4PSK} = [\theta_1 \ \pi - \theta_1 \ \pi + \theta_1 \ 2\pi - \theta_1]$ as the basis. By applying the recursive algorithm to (7) and (9), they can be

rewritten as

$$\begin{aligned} & \Psi_{H-8PSK} \\ &= [\theta_1 - \theta_2 \ \theta_1 + \theta_2 \ \pi - \theta_1 - \theta_2 \ \pi - \theta_1 + \theta_2 \ \pi + \theta_1 - \theta_2 \\ & \quad \pi + \theta_1 + \theta_2 \ 2\pi - \theta_1 - \theta_2 \ 2\pi - \theta_1 + \theta_2] \\ &= \Delta \left\{ \Psi_{H-4PSK} \Big|_{\theta_1 \leftarrow \theta_1 + \theta_2}, \Psi_{H-4PSK} \Big|_{\theta_1 \leftarrow \theta_1 - \theta_2} \right\} \quad (21) \end{aligned}$$

and

$$\begin{aligned} & \Psi_{H-16PSK} \\ &= [\theta_1 - \theta_2 - \theta_3 \ \theta_1 - \theta_2 + \theta_3 \ \theta_1 + \theta_2 - \theta_3 \ \theta_1 + \theta_2 + \theta_3 \\ & \quad \pi - \theta_1 - \theta_2 - \theta_3 \ \pi - \theta_1 - \theta_2 + \theta_3 \ \pi - \theta_1 + \theta_2 - \theta_3 \ \pi - \theta_1 + \theta_2 + \theta_3 \\ & \quad \pi + \theta_1 - \theta_2 - \theta_3 \ \pi + \theta_1 - \theta_2 + \theta_3 \ \pi + \theta_1 + \theta_2 - \theta_3 \ \pi + \theta_1 + \theta_2 + \theta_3 \\ & \quad 2\pi - \theta_1 - \theta_2 - \theta_3 \ 2\pi - \theta_1 - \theta_2 + \theta_3 \ 2\pi - \theta_1 + \theta_2 - \theta_3 \ 2\pi - \theta_1 + \theta_2 + \theta_3] \\ &= \Delta \left\{ \Psi_{H-8PSK} \Big|_{\theta_2 \leftarrow \theta_2 + \theta_3}, \Psi_{H-8PSK} \Big|_{\theta_2 \leftarrow \theta_2 - \theta_3} \right\}, \quad (22) \end{aligned}$$

respectively. When $\Psi^X = [\psi_1^X \ \psi_2^X \ \psi_3^X \ \dots]$ and $\Psi^Y = [\psi_1^Y \ \psi_2^Y \ \psi_3^Y \ \dots]$, $\Delta \{ \Psi^X, \Psi^Y \}$ is defined by

$$\Delta \{ \Psi^X, \Psi^Y \} = \begin{cases} [\psi_1^Y \ \psi_1^X \ \psi_2^Y \ \psi_2^X \ \psi_3^Y \ \psi_3^X \ \dots], & m = \text{odd} \\ [\psi_1^X \ \psi_1^Y \ \psi_2^Y \ \psi_2^X \ \psi_3^X \ \psi_3^Y \ \dots], & m = \text{even}. \end{cases} \quad (23)$$

Finally, from (21) and (22), the phase vector for H-MPSK is obtained as

$$\begin{aligned} & \Psi_{H-MPSK} \\ &= \Delta \left\{ \Psi_{H-\frac{M}{2}PSK} \Big|_{\theta_{m-2} \leftarrow \theta_{m-2} + \theta_{m-1}}, \Psi_{H-\frac{M}{2}PSK} \Big|_{\theta_{m-2} \leftarrow \theta_{m-2} - \theta_{m-1}} \right\}, \quad (24) \end{aligned}$$

and the angle pairs for $b_k, k \geq 3$ can be more easily obtained as follows:

for b_3 , and $n = 0, 1, \dots, l-1$,

$$\begin{pmatrix} \phi_1 \\ \phi_2 \end{pmatrix} = \begin{cases} \begin{pmatrix} \psi_{2n} |_{H-2^{k-1}PSK} \\ \psi_{2n+1} |_{H-2^{k-1}PSK} \end{pmatrix}, & \text{when } b_3 = 1, \\ \begin{pmatrix} \psi_{2n+1} |_{H-2^{k-1}PSK} \\ \psi_{2n+2} |_{H-2^{k-1}PSK} \end{pmatrix}, & \text{when } b_3 = 0; \end{cases} \quad (25)$$

for b_k , ($k > 3$) and $n = 0, 1, \dots, l-1$.

$$\begin{pmatrix} \phi_1 \\ \phi_2 \end{pmatrix} = \begin{cases} \begin{pmatrix} \psi_{2n} |_{H-2^{k-1}PSK} \\ \psi_{2n+1} |_{H-2^{k-1}PSK} \end{pmatrix}, & \text{when } b_k (k > 3) = 0, \\ \begin{pmatrix} \psi_{2n+1} |_{H-2^{k-1}PSK} \\ \psi_{2n+2} |_{H-2^{k-1}PSK} \end{pmatrix}, & \text{when } b_k (k > 3) = 1. \end{cases} \quad (26)$$

6. Average BER Expression of H-MPSK

An average BER expression over N bits of H-MPSK can be obtained as

$$P(e) = \frac{1}{N} \sum_{k=1}^N P_b(k), \quad (27)$$

where $P_b(k)$ is the BER of the k -th bit, which can be obtained by

$$P_b(k) = \frac{1}{M} \sum_{j=0}^{M-1} \sum_{n=0}^{l-1} Q \left(-\frac{E[Y_1]}{\sqrt{\text{Var}[Y_1]}}, \frac{E[Y_2]}{\sqrt{\text{Var}[Y_2]}}; -\rho_{Y_1 Y_2} \right). \quad (28)$$

The arguments of the Q-function in (28) can be obtained from (2) with the signal phases and angle pairs given in (15)-(19).

Another BER expression for H-MPSK can be obtained by applying equation (9) in [13] to equation (14) in [13]. The resulting expression differs from the final expressions (27) and (28) in this paper, which are obtained by finding the regular patterns of the phase information, namely, the phase (ψ_j) and angle pairs (ϕ_1, ϕ_2). The changeable phase information is not obtained from the method provided in [13]. Also, when equation (14) of [13] is used, we require the $M(M-1)$ statistical calculations of (2) to get the BER results, but the results of (27) and (28) can be obtained from only the $M \cdot \sum_k l$ calculations.

Calculation of the BER results for H-MPSK from (27) and (28) is consequently less complex and time-consuming than from equation (14) in [13].

IV. Numerical Results and Analysis

The evaluation of the numerical results for the provided BER

expression is compared and analyzed based on two criteria. For I/Q balance, our BER results are compared to those of [2], and for I/Q imbalances, the effect of I/Q imbalances on the BER performance of H-MPSK is investigated. To this end, H-16PSK with $\Theta_{16} = [\pi/4.2, \pi/8.6, \pi/17.5]$ is considered, and the values of parameters $\phi_R = 5^\circ$ and $r=0.9, 1.1$ are used since typical values achievable with careful design are $\phi_R = 5^\circ$ and α or $\beta=1.1$ [12], where $r = \alpha/\beta$ is the gain ratio [19].

First, for I/Q balanced H-16PSK with $\Theta_{16} = [\pi/4.2, \pi/8.6, \pi/17.5]$, the BER results obtained by (27) and (28) are compared with the results of [2]. As shown in Fig. 6, although the final expressions of this paper and [2] differ, we can confirm that the numerical results of both are clearly the same. Figure 7 shows the BER for I/Q balanced H-16PSK and

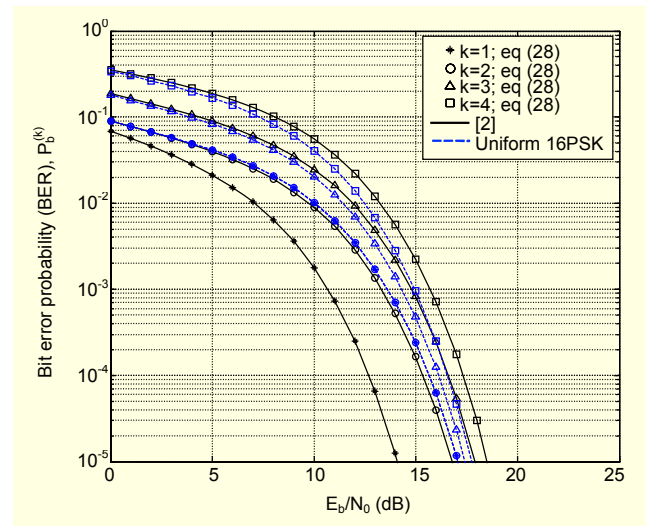


Fig. 6. Comparison of the results of (28) with the results of [2] for I/Q balance.

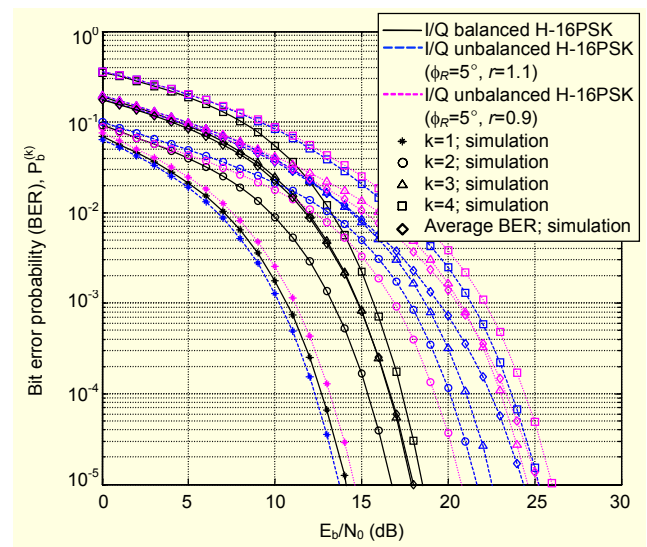


Fig. 7. Effect of I/Q imbalances on the BER of H-16PSK.

I/Q unbalanced H-16PSK with $\phi_r = 5^\circ$ and $r = 0.9, 1.1$. As shown in Fig. 7, for $r=1.1$, since the minimum distances between the decision boundary of the first bit (b_1) and the signal points increase as I/Q imbalances increase, the BER of the first bit for the I/Q unbalanced H-16PSK is gradually improved. However, the average BER is degraded as I/Q imbalances increase, because the BERs of other bits ($b_k, k=2, 3, 4$) for I/Q unbalanced H-16PSK are degraded. For $r = 0.9$, the minimum distances between the decision boundary of the first bit (b_1) and the signal points decrease as I/Q imbalances increase. Thus, the BERs and average BER of all bits ($b_k, k=1, 2, 3, 4$), including the first bit, are degraded as I/Q imbalances increase. Figure 7 also shows the effect of I/Q imbalances on the BER performance of an H-MPSK system to be quite serious for all but the first bit (b_1). Figure 7 also shows excellent agreement between the results of the analytical expression and the Monte Carlo simulation.

V. Conclusion

In this paper, we provided a new closed-form expression involving the two-dimensional Gaussian Q-function for the BER of H-MPSK with I/Q phase and amplitude imbalances over the AWGN channel. We first obtained the phases of all transmitted signal points and the angle pairs for the k -th bit of the signal points in H-4/8/16PSK. We then observed the regular patterns of varying angle values. Finally, we provided the exact and general BER expression of H-MPSK based on the observed patterns. The provided BER expression for H-MPSK with I/Q phase and amplitude imbalances can be readily applied in numerical evaluation of various cases of practical interest of unbalanced I/Q H-MPSK systems. This positive attribute is afforded by the common availability of mathematical software packages capable of directly computing the two-dimensional Gaussian Q-function, and because the phases and angle pairs which vary with the positions of signal points can be simply obtained using the function provided to generate a regular pattern and a recursive algorithm.

References

- [1] T. Cover, "Broadcast Channels," *IEEE Trans. Inform. Theory*, vol. IT-18, Jan. 1972, pp. 2-14.
- [2] P.K. Vitthaladevuni and M.S. Alouini, "Exact BER Computation of Generalized Hierarchical PSK Constellations," *IEEE Trans. Commun.*, vol. 51, no. 12, Dec. 2003, pp. 2030-2037.
- [3] *Digital Video Broadcasting; Framing Structure, Channel Coding and Modulation for Terrestrial Television*, ETSI, EN300 744, vol.1.2, 1997.
- [4] *DVB-T Standard: ETS 300 744, Digital Broadcasting Systems for Television, Sound and Data Services: Framing Structure, Channel Coding and Modulation for Digital Terrestrial Television*, ETSI Draft, vol. 1.2.1, no. EN300 744, 1999.
- [5] *Digital Video Broadcasting; Second Generation Framing Structure, Channel Coding and Modulation Systems for Broadcasting, Interactive Services, News Gathering, and Other Broadband Satellite Applications*, ETSI, EN 302 307, vol. 1.1.1, 2005.
- [6] *Digital Video Broadcasting (DVB): User Guidelines for the Second Generation System for Broadcasting, Interactive Services, News Gathering, and Other Broadband Satellite Applications (DVB-S2)*, ETSI, TR 102 376, vol. 1.1.1, 2005.
- [7] M.B. Pursley and J.M. Shea, "Non-uniform Phase-Shift-Key Modulation for Multimedia Multicast Transmission in Mobile Wireless Networks," *IEEE J. Select. Areas Commun.*, vol. SAC-17, May 1999, pp. 774-783.
- [8] M.B. Pursley and J.M. Shea, "Adaptive Non-uniform Phase-Shift-Key Modulation for Multimedia Traffic in Wireless Networks," *IEEE J. Select. Areas Commun.*, vol. SAC-00, Aug. 2000, pp. 1394-1407.
- [9] P.K. Vitthaladevuni and M.S. Alouini, "BER Computation of 4/M QAM Hierarchical Constellations," *IEEE Trans. on Broadcasting*, vol. 47, no. 3, Sept. 2001, Sept. 2001, pp. 228-239.
- [10] P.K. Vitthaladevuni and M.S. Alouini, "A Recursive Algorithm for the Exact BER Computation of Generalized Hierarchical QAM Constellations," *IEEE Trans. on Inform. Theory*, vol. 49, no. 1, Jan. 2003, pp. 297-307.
- [11] R.F. Pawula, S.O. Rice, and J.H. Roberts, "Distribution of the Phase Angle Between Two Vectors Perturbed by Gaussian Noise," *IEEE Trans. Commun.*, vol. 30, Aug. 1982, pp. 1828-1841.
- [12] C. Rorabaugh, *Simulating Wireless Communication Systems: Practical Models in C++*, Prentice Hall, 2004.
- [13] J. Lee, D. Yoon, and K. Hyun, "Exact and General Expression for the Error Probability of Arbitrary Two-Dimensional Signaling with I/Q Amplitude and Phase Unbalances," *IEICE Trans. Commun.*, vol. E89-B, no. 12, Dec. 2006, pp. 3356-3362.
- [14] M. Abramowitz and I.A. Stegun, *Handbook of Mathematical Functions with Formulas, Graphs, and Mathematical Tables*, National Bureau of Standards Applied Mathematics Series: U.S. Department of Commerce, 1982.
- [15] S. Park and D. Yoon, "An Alternative Expression for the Symbol Error Probability of MPSK in the Presence of I/Q Unbalance," *IEEE Trans. Commun.*, vol. 52, no. 12, Dec. 2004, pp. 2079-2081.
- [16] M.K. Simon and D. Divsalar, "Some New Twists to Problems Involving the Gaussian Probability Integral," *IEEE Trans. Commun.*, vol. 46, Feb. 1998, pp. 200-210.
- [17] K. Cho and D. Yoon, "On the General BER Expression of One and Two Dimensional Amplitude Modulations," *IEEE Trans. Commun.*, vol. 50, July 2002, pp. 1074-1080.

- [18] Visual Numerics, Inc., *IMSL C Numerical Library (CNL) User's Guides*, version 5.5, retrieved from: <http://www.vni.com/products/imsl/documentation/index.html>, 2003.
- [19] J.K. Caver and M.W. Liao, "Adaptive Compensation for Unbalance and Offset Losses in Direct Conversion Transceivers," *IEEE Trans. Veh. Technol.*, vol. 42, no. 4, Nov. 1993, pp. 581-588.



Jaeyoon Lee received the BS and MS degrees from the Department of Information and Communications Engineering of Daejeon University, Daejeon, Rep. of Korea, in 2002 and 2004, respectively. He is currently working toward a PhD degree in the Department of Electronics and Computer Engineering of Hanyang University, Seoul, Rep. of Korea. His research interests lie in the field of new modulation techniques, accurate performance evaluations and digital communications theory.



Kyongkuk Cho received the BS and MS degrees from Hanyang University, Seoul, Rep. of Korea, in 1995 and 1997, respectively. From January 1997 to March 2006, he was a research engineer in LG Electronics Inc., Seoul, Rep. of Korea. Currently, he is a PhD student at Hanyang University, Seoul, Rep. of Korea. His research interests are in modulation, wireless communication, ASIC/ modem architecture, and 4th generation wireless communications.



Dongweon Yoon received the BS (summa cum laude), MS, and PhD degrees in electronic communications engineering from Hanyang University, Seoul, Rep. of Korea, in 1989, 1992 and 1995. From March 1995 to August 1997, he was an assistant professor in the Department of Electronic and Information Engineering of Dongseo University, Pusan, Rep. of Korea. From September 1997 to February 2004, he was an associate professor in the Department of Information and Communications Engineering of Daejeon University, Daejeon, Rep. of Korea. Since March 2004, he has been on the faculty of Hanyang University, Seoul, Rep. of Korea, where he is now an associate professor in the Department of Electronics and Computer Engineering. He has twice been an invited researcher at the Electronics and Telecommunications Research Institute (ETRI), Daejeon, Rep. of Korea (February to December 1997 and November 2002 to December 2005). He was a visiting professor at the Pennsylvania State University, University Park, Pennsylvania, for the academic year from 2001 to 2002. He has served as a consultant for a number of companies and given many lectures on the topics of digital communications and wireless communications. His research interests include new modulation techniques, accurate performance evaluations, digital communications theory and system, spread spectrum communications, and wireless communications.